

CHOICE OF INITIAL OPERATING PARAMETERS FOR HIGH AVERAGE
CURRENT LINEAR ACCELERATORS

Kenneth Batchelor
Brookhaven National Laboratory
Upton, New York 11973

NOTICE
This report was prepared as an account of work sponsored by the United States Government. Neither the United States nor the United States Energy Research and Development Administration, nor any of their employees, nor any of their contractors, subcontractors, or their employees, makes any warranty, express or implied, or assumes any legal liability or responsibility for the accuracy, completeness or usefulness of any information, apparatus, product or process disclosed, or represents that its use would not infringe privately owned rights.

1. Introduction

Recent emphasis on alternative energy sources together with the need for intense neutron sources for testing of materials for CTR has resulted in renewed interest in high current (~100 mA) c.w. proton and deuteron linear accelerators. (1-7) In designing an accelerator for such high currents it is evident that beam losses in the machine must be minimized, which implies well matched beams, and that adequate acceptance under severe space charge conditions must be met. This paper investigates the input parameters to an Alvarez type drift-tube accelerator resulting from such factors.

2. Theory

A number of authors have investigated the effects of space charge on injection for existing proton linear accelerators (8-14) using as models either a uniformly charged ellipsoid or infinitely long elliptical cylinder. It has been shown (15) that the ellipsoidal model tends to give pessimistic results in terms of maximum acceptance without beam loss but is a useful analytical tool for comparative data so it will be used in this analysis.

Assuming that the beam bunch is a uniformly charged ellipsoid, one can write the non-relativistic beam envelope equations (14) taking the smooth approximation for the transverse motion as:

$$\frac{d^2 a}{dn^2} + K_t^2 \beta^2 \lambda^2 \cdot a - \frac{P^2}{a^3} = \mu \cdot \frac{[1-f(a)]}{2ab} \quad (1)$$

$$\frac{d^2 b}{dn^2} + K_l^2 \beta^2 \lambda^2 \cdot b - \frac{Q^2}{b^3} = \mu \cdot f\left(\frac{b}{a}\right) \quad (2)$$

$dn = \frac{ds}{\beta\lambda}$ (λ is the rf wavelength and s is the distance along the linac axis both in meters).

$$\mu = \frac{90 e I \lambda^3}{m_o c^2}$$

a is the average beam radius in meters ($a = \sqrt{a_x a_y}$)

where $2 a_x$ and $2 a_y$ are the width of the beam in the x and y directions. At a symmetry point in an x-focusing and y defocusing quadrupole magnet

$\frac{x}{a} = \Psi$, where Ψ is obtained from the radial stability diagram of Smith and Gluckstern. (16)

$2b$ is the bunch length in meters.
 K_t is the wave number in meter⁻¹ of the transverse particle oscillations in the zero space charge approximation. ($K_t = \frac{\mu_{sf}}{2\beta\lambda}$ where μ_{sf} is the phase advance of the transverse particle oscillation per magnet period for zero beam current assuming +--+ quadrupole configuration).

K_l is the wave number in meter⁻¹ of the longitudinal particle oscillation in the zero space charge approximation $K_l = \left[\frac{2\pi E_o T \sin |\phi|}{m_o c^2 \lambda \beta^3} \right]^{1/2}$ where

$$K_l = \left[\frac{2\pi E_o T \sin |\phi|}{m_o c^2 \lambda \beta^3} \right]^{1/2}$$

*Work performed under the auspices of the U.S. Energy Research and Development Administration

E_o is the average electric field in volts/m. T is the transit time factor, ϕ_s is the synchronous phase). $m_o c^2$ is the deuteron rest mass in electron volts. P is the area of the beam in π meter² in the $a, da/dn$ space. Q is the area of the beam in π meter² in the $b, db/dn$ space and is proportional to the conventional longitudinal emittance in $\Delta\gamma-\Delta\phi$ space ($Q = \frac{3\phi_s}{2} \times \frac{\beta\lambda}{2\pi} \times \frac{\lambda\Delta\gamma}{\beta\gamma^3}$ for beam of width $3\phi_s$ and energy spread corresponding to $\pm \Delta\gamma$). I is the beam current in amperes.

$f\left(\frac{b}{a}\right)$ is a form factor for the ellipsoid and can be approximated by $\frac{a}{3b}$ for $1 < \frac{b}{a} < 5$.

for matched conditions $\frac{d^2 a}{dn^2} \approx 0$ and $\frac{d^2 b}{dn^2} \approx 0$.

Giving for $f\left(\frac{b}{a}\right) \approx \frac{a}{3b}$

$$K_t^2 \beta^2 \lambda^2 - \frac{P^2}{a^4} = \frac{\mu(3b-a)}{6a^2 c^2} \quad (3)$$

$$K_l^2 \beta^2 \lambda^2 - \frac{Q^2}{b^4} = \frac{\mu}{3ab^2} \quad (4)$$

These can be rewritten as:

$$K_t'^2 \beta^2 \lambda^2 = \frac{P^2}{a^4} \quad (5)$$

$$K_l'^2 \beta^2 \lambda^2 = \frac{Q^2}{b^4} \quad (6)$$

where $K_t'^2 = K_t^2(1-\mu_t)$ and $K_l'^2 = K_l^2(1-\mu_l)$ where K_t', K_l' are the modified wave numbers in the radial and longitudinal directions in the presence of space charge and μ_t and μ_l are the ratios of the space charge defocusing force to the restoring force in those directions. It can be seen that

$$\mu_t = \frac{\mu(3b-a)}{6K_t^2 \beta^2 \lambda^2 a^2 b^2} \quad (7)$$

$$\text{and } \mu_l = \frac{\mu}{3K_l^2 \beta^2 \lambda^2 ab^2} \quad (8)$$

or substituting for μ, K_t and K_l

$$\mu_t = \frac{60e}{m_o c^2} I \frac{\left(\frac{3b}{\lambda} - \frac{a}{\lambda}\right)}{\mu_{sf}^2 \left(\frac{a}{\lambda}\right)^2 \left(\frac{b}{\lambda}\right)^2} \quad (9)$$

$$\mu_l = \frac{15 \cdot I \cdot \beta}{\pi E_o T \sin |\phi_s| \cdot \lambda \left(\frac{a}{\lambda}\right) \left(\frac{b}{\lambda}\right)^2} \quad (10)$$

where $\frac{b}{\lambda} = \frac{\beta(\phi-\phi_s)}{2\pi}$.

MASTER EP

DISTRIBUTION OF THIS DOCUMENT IS UNLIMITED

DISCLAIMER

This report was prepared as an account of work sponsored by an agency of the United States Government. Neither the United States Government nor any agency Thereof, nor any of their employees, makes any warranty, express or implied, or assumes any legal liability or responsibility for the accuracy, completeness, or usefulness of any information, apparatus, product, or process disclosed, or represents that its use would not infringe privately owned rights. Reference herein to any specific commercial product, process, or service by trade name, trademark, manufacturer, or otherwise does not necessarily constitute or imply its endorsement, recommendation, or favoring by the United States Government or any agency thereof. The views and opinions of authors expressed herein do not necessarily state or reflect those of the United States Government or any agency thereof.

DISCLAIMER

Portions of this document may be illegible in electronic image products. Images are produced from the best available original document.

Study of relationships (9) and (10) remembering that $\frac{b}{\lambda} \propto \beta$ shows the following:

(a) The higher the input β and hence input energy the smaller the radial and longitudinal space charge forces relative to the restoring forces.

(b) The higher the current the higher the space charge forces relative to the restoring forces.

(c) The larger the phase advance per magnet period the lower the space charge to restoring force ratio in the radial direction. (Note that μ_{sf} may not exceed π if radial stability is to be maintained so this sets an upper limit to the initial quadrupole focusing field.)

(d) The longer the rf wavelength or the lower the rf frequency the smaller the ratio of longitudinal space charge force to restoring force.

(e) The higher the average acceleration rate ($=E_0 T \cos |\phi_s|$) the smaller the ratio of longitudinal space charge force with respect to the restoring force. (Since the maximum attainable electric field gradient varies as λ^{-2} this conflicts with condition (d) above).

(f) The larger the stable phase angle the smaller the longitudinal space charge to restoring force ratio.

3. Practical Considerations

In a practical design the maximum acceptable current may be limited by factors other than space charge. For example, there is an upper limit to the electric field gradient and quadrupole field gradient both of which are frequency dependent. The total beam emittance from the pre-accelerator and low energy beam transport system will also influence the results. In addition, for a given frequency or wavelength, there is a practical upper limit to the drift tube aperture resulting from transit time considerations.

For this report an injection energy of 750 KeV has been used as a compromise between these various factors. For practical transit time factors this limits the aperture radius to about 6.7×10^{-3} wavelength. Having selected the injection energy and maximum aperture the maximum acceleration rate is determined by the sparking limit. Taking Kilpatrick's data as a criterion this implies a maximum acceleration rate of 1.6 MeV/m at a wavelength of 1.5 meters for a stable phase angle of 40° . Space charge considerations indicate that the highest practical acceleration rate and stable phase should be used for maximum acceptance so this value has been chosen for the design. The electric field breakdown limit varies as λ^{-2} giving an acceleration rate of 1.12 MeV/m at $\lambda = 6m$.

The longitudinal emittance of the input beam is determined largely by the bunching scheme used since the beam from the d.c. pre-accelerator has essentially zero longitudinal emittance. It has been assumed that the phase width of the input beam can be made equal to $\pm\phi_s$ and that the energy spread can be made equal to the "matched" energy spread given by

$$\Delta E = \pm m_0 c^2 \beta^2 b K_L (1 - \mu_L) \text{ where } b = \phi_s \times \frac{\beta \lambda}{2\pi}$$

μ_L is assumed to be about 0.75.

These considerations define the longitudinal input beam parameters given in Table I.

Given these parameters and a value for the radial emittance it is now possible to optimize the acceptance by varying the quadrupole gradient within the practical limits of attainable quadrupole gradient and radially stability.⁽¹⁶⁾ Radially stability is determined by the operating point on the stability diagram (Fig. 1) under space charge conditions. For a given quadrupole gradient the operating point for the reference particle moves towards the $\mu_{sf} = +1$ stability limit as the space charge force increases.

For a given injection energy, increasing the wavelength clearly reduces the required quadrupole gradient due to the greater drift tube length available, but at the same time increases the r.f. defocusing force thus requiring stronger focusing fields. A non-normalized radial emittance of (I) $3.7 \pi \times 10^{-4}$ m. rad. was chosen for the reference design where I is the beam current in amperes. This value is a conservative estimate based on measured values for pulsed proton currents of up to 400 mA.

5. Numerical Results

Interest at Brookhaven has centered on a 1 GeV proton linac with a beam current of 300 mA and a deuteron accelerator of 35 MeV energy and 200 mA beam current. For the deuteron machine the effect of injection energy on the acceptance was investigated at a wavelength of 3 meters or frequency of 50 MHz. The bore radius was allowed to increase with energy roughly as β so that the aperture at 750 KeV is 4.8 cm compared with 4 cm at 500 KeV and 3.5 cm at 350 KeV. This is a conservative choice and as can be seen from Fig. 2, gives rise to quadrupole fields which are readily attainable. Fig. 3 shows the matched beam parameters for deuterons of different energies for three different initial quadrupole field gradients. The optimum attainable beam current at a given injection energy is obtained when the radial and longitudinal acceptance limits are reached at the same time. This is achieved by allowing the initial electric and magnetic quadrupole field gradients to vary within the acceptable stability limits and practical quadrupole magnetic field and electrical sparking limits. Thus, in Fig. 2 the maximum attainable beam current without loss is plotted as a function of injection energy for a deuteron beam of constant longitudinal emittance of $6\pi \times 10^{-4}$ m. rad and a radial emittance given by $I \times 3\pi \times 10^{-4}$ m. rad where I is the beam current in amperes. For protons, with their higher β value, it is possible to increase the drift-tube aperture by almost a factor of 2 and thus accept a larger beam current for the same emittance value. Here the radial acceptance limit is defined as that point at which the flutter factor causes the beam to occupy 2/3 of the drift-tube aperture.

The influence of wavelength or frequency on the matched beam parameters for protons using the longitudinal emittance values given in Table I, with a radial emittance of $1.11 \pi \times 10^{-4}$ m. rad, and a beam current of 300 mA is plotted in Fig. 4. It shows a gradual increase in the beam radius and beam length to wavelength ratios with increasing frequency. The phase advance per magnetic period was held constant at $\frac{\pi}{2}$ for zero current in order to compute this set of curves. The increase in a/λ and b/λ would be greater (approximately increasing as $f^{3/2}$), if the longitudinal emittance was held constant.

Figures 5 and 6 show the matched beam parameters as a function of beam current for deuterons and protons respectively. The injection energy used is 750 KeV in both cases and the operating frequency is 50 MHz. Note that the higher β value and hence larger aperture for protons allows currents of up to 1.2 amperes in the proton case compared with 0.4 amperes for deuterons. Calculations indicate that even at a frequency of 200 MHz it is possible to accept 0.4 A of proton current but the quadrupole field strength required is high (13.5 KG/cm) and is probably at the practical limit for conventional quadrupoles.

The effect of longitudinal emittance on the matched beam parameters is shown in Fig. 7 for a 0.2 ampere deuteron current of 750 KeV energy at a wavelength of 6 m. Fig. 8 shows the corresponding effect of radial emittance for deuterons.

The effect of longitudinal and radial emittance on the matched beam parameters for a 750 KeV proton beam current of 0.3 amperes is shown in Figs. 9 and 10 for wavelengths of 1.5 m, 3 m and 6 m.

5. Conclusions

The analysis indicates that an accelerator operating at a frequency of 50 MHz is capable of accepting deuteron currents of about 0.4 amperes and proton currents of about 1.2 amperes. These values depend critically on the assumed values of beam emittance and on the ability to properly "match" this to the linac acceptance.

The analysis does not concern itself with acceleration so none of the growth effects arising therefrom are considered. These effects and the effects of misalignments and quadrupole and electric field gradient errors may further limit the acceptable beam current. A detailed computer study will be necessary to determine the full validity of the above.

6. Acknowledgement

The author recognizes the previous work of Professor R.L. Gluckstern and Dr. R. Chasman and is indebted to P. Grand for many helpful discussions.

References

1. P. Grand et al., Proposal for an Accelerator Based Neutron Generator, July 1975, BNL 20159.
2. P. Grand et al., Addendum to above report, January 1976, BNL 20840.
3. M.J. Saltmarsh and R.E. Worsham, Ingrid an Intense Neutron Generator for Radiation Induced Damage Studies in the CTR Materials Program, October 1975, ORNL 5098.
4. HEDL Staff - CTR Materials Irradiation Testing Facility (CMIT), November 1975.
5. Joint Proposal by Lawrence-Livermore and Lawrence-Berkeley Laboratories for High Intensity Neutron Source, January 1976.
6. W. Bennet Lewis, Immediate Relation of ING to Fast Breeder Reactor Programs, January 1969, AECL-3251.
7. Meyer Steinbert et al., The Clean Breeder Machine (CBM), Internal Report, Brookhaven National Laboratory, March 1976.
8. I.M. Kapchinsky and V.V. Vladimirovsky, Conference of High Energy Accelerators and Instrumentation, CERN, Geneva (1959), p.274.
9. P.L. Morton, Review of Scientific Instruments, 36, 1826 (1965).
10. R.L. Gluckstern, Proceedings of 1966 Linear Accelerator Conference, October 3-7, 1966, LA-3609, p.220.
11. T. Nishikawa, SJC, A-67-1, University of Tokyo, (June 1967).
12. P.M. Labostolle, CERN Report ISR-300, LIN 166-32, October, 1966.
13. S. Ohnuma, Proceedings of 1966 Linear Accelerator Conference, LASL, October 3-7, 1966, LA-3609, p.220.
14. R. Chasman, Proceedings of 1968 Linear Accelerator Conference, May 20-24, 1968, Brookhaven National Laboratory, BNL 50120 (C-54).
15. A. Barton, R. Chasman, C. Agritellis, IEEE Transactions on Nuclear Science, June 1967, Vol. NS-14, Number 3, p. 507.
16. R.L. Gluckstern and L. Smith, Review of Scientific Instruments, Vol. 26, No. 2, February 1955, p.220.

TABLE I

Frequency MHz	Wavelength Meters	Energy Spread (ΔE)MeV	Δy	Longitudinal Emittance M. rad	Q π Meter ²	K ² Meter ⁻¹
50	6	± 0.034	3.65×10^{-5}	$9.12\pi \times 10^{-4}$	2.19	0.0342
100	3	± 0.029	3.06×10^{-5}	$3.82\pi \times 10^{-4}$	0.458	0.0573
200	1.5	± 0.024	2.58×10^{-5}	$1.61\pi \times 10^{-4}$	0.097	0.0968

Figure Captions

- Figure 1 Radial Stability Diagram
- Figure 2 Maximum Accepted Beam Current as a Function of Injection Energy
- Figure 3 Matched Beam Parameters as a Function of Injection Energy
- Figure 4 Matched Beam Parameters as a Function of Frequency for a Proton Beam Current of 0.3 Amperes
- Figure 5 Matched Beam Parameters as a Function of 750 KeV Deuteron Beam Current
- Figure 6 Matched Beam Parameters as a Function of 750 KeV Proton Beam Current
- Figure 7 Matched Beam Parameters as a Function of Longitudinal Emittance for a 750 KeV Deuteron Beam Current of 0.2 Amperes
- Figure 8 Matched Beam Parameters as a Function of Radial Emittance for a 750 KeV Deuteron Beam Current of 0.2 Amperes
- Figure 9 Matched Beam Parameters as a Function of Longitudinal Emittance for a 750 KeV Proton Beam Current of 0.3 Amperes
- Figure 10 Matched Beam Parameters as a Function of Radial Emittance for a 750 KeV Proton Beam Current of 0.3 Amperes

Figure 1

- o - OPERATING POINT FOR STABLE PARTICLE WITHOUT SPACE CHARGE ($I_b = 0$)
 - x - OPERATING POINT FOR STABLE PARTICLE WITH SPACE CHARGE ($I_b = 0.3A$)
- $E_{INJ} = 750 \text{ KeV}$ $\mu_{sf} = \pi/2$

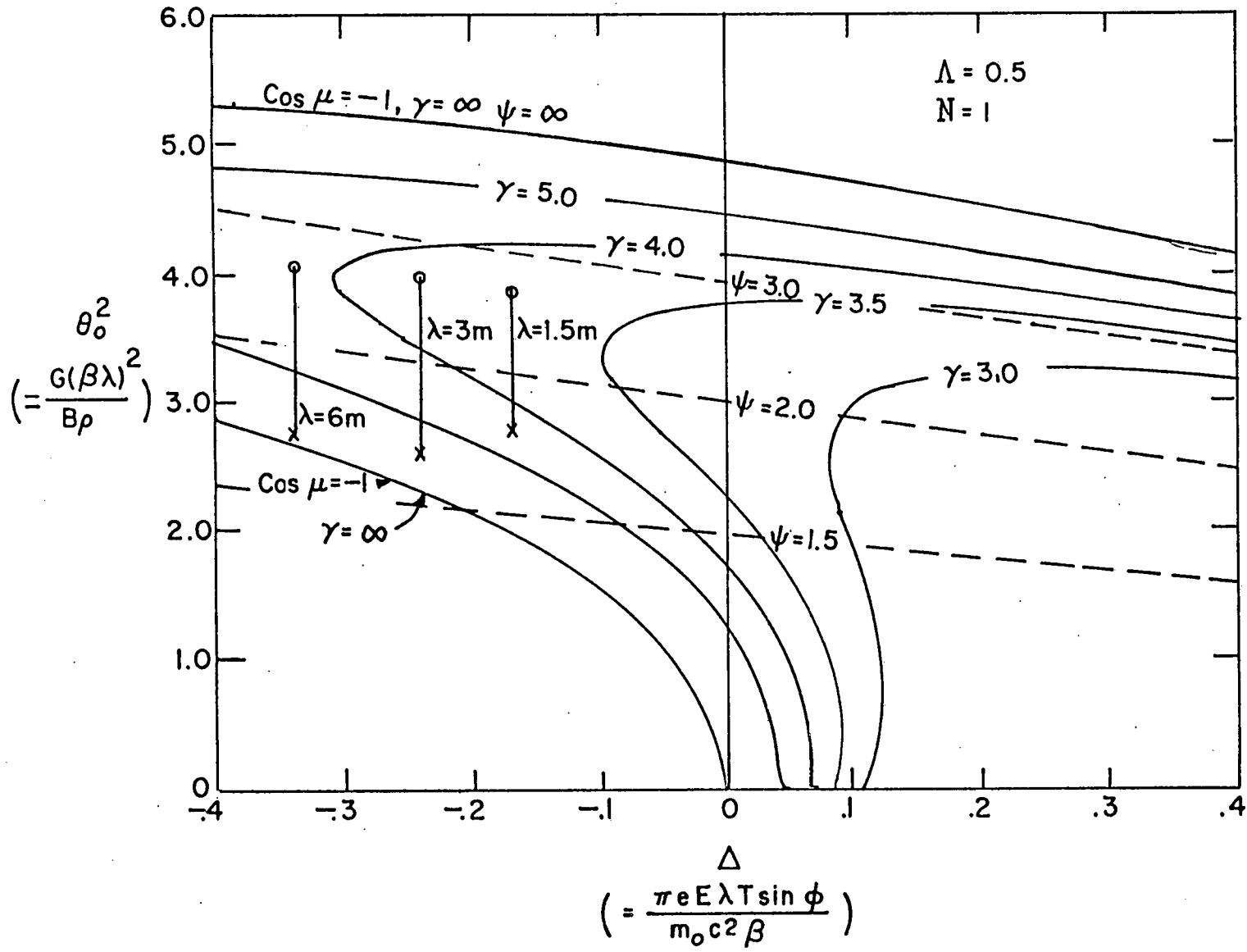


Figure 2

MATCHED BEAM PARAMETERS AS A FUNCTION OF INJECTION ENERGY FOR DIFFERENT INITIAL QUADRUPOLE GRADIENTS WITH $+-+-$ QUADRUPOLE CONFIGURATION, MAGNET LENGTH/CELL LENGTH = 0.5, BORE RADIUS = 2 cm, $\lambda = 6$ m, ACCELERATION RATE = 1 MeV/m, $\phi_s = 35^\circ$, BEAM CURRENT = 0.2 A, RADIAL EMITTANCE = $6\pi \times 10^{-4}$ m-rad, LONGITUDINAL EMITTANCE $6\pi \times 10^{-4}$ m-rad DEUTERONS

x - $G_i = 2.4$ kG/cm • - $G_i = 3$ kG/cm Δ - $G_i = 4$ kG/cm

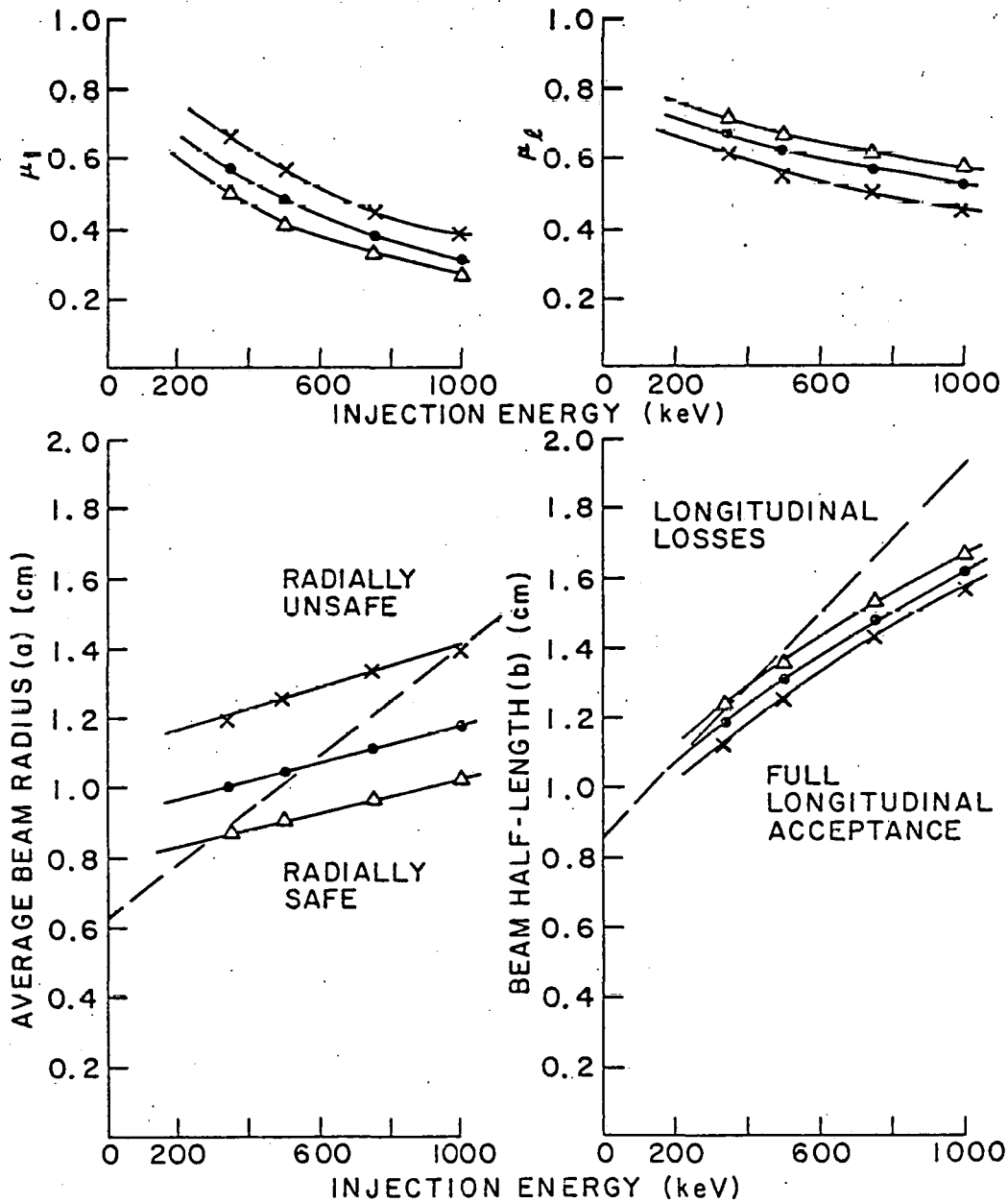


Figure 3

MAXIMUM ACCEPTED BEAM CURRENT AS A FUNCTION OF INJECTION ENERGY. ACCELERATION RATE = 1 MeV/m
 $\phi_s = 35^\circ$, MAGNET LENGTH/CELL LENGTH = 0.5 WITH
+ - + - QUADRUPOLE CONFIGURATION, $\lambda = 6\text{m}$, BORE RADIUS INCREASING WITH β FROM 1.25cm AT 350 keV TO 2.5cm AT 750 keV, LONGITUDINAL EMITTANCE = $6\pi \cdot 10^{-4}\text{m-rad}$, RADIAL EMITTANCE = $1.3\pi \cdot 10^{-4}\text{m-rad}$.
(I IS BEAM CURRENT IN AMPS) DEUTERONS

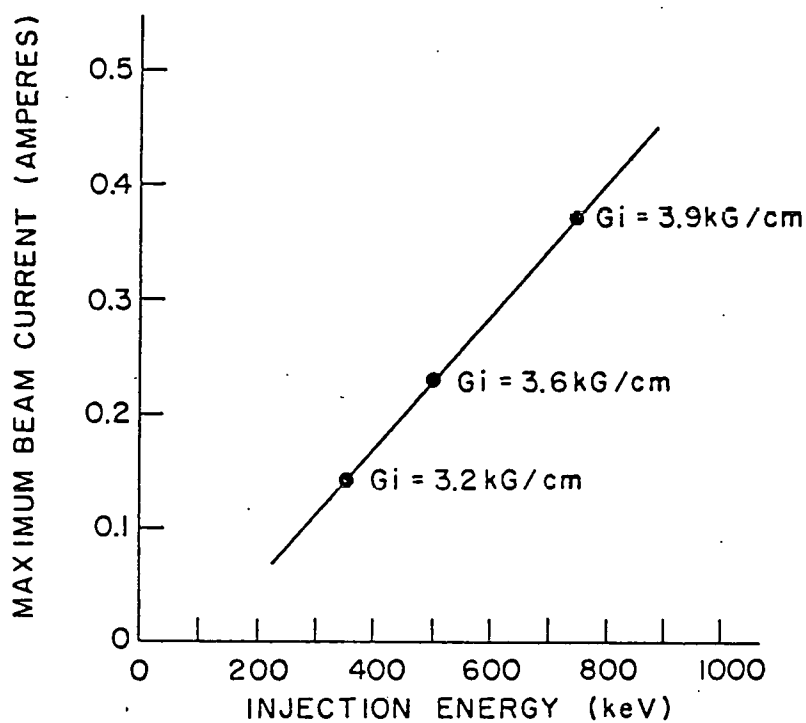


Figure 4

MATCHED BEAM PARAMETERS AS A FUNCTION OF FREQUENCY FOR 750 keV PROTON CURRENT OF 0.3 A for +--+ QUADRUPOLE CONFIGURATION AND CONSTANT PHASE ADVANCE PER MAGNET PERIOD = $\pi/2$. MAGNET /CELL LENGTH = 0.5; BORE RADIUS/WAVE LENGTH = 6.667×10^{-3} , $\phi_s = 40^\circ$, MAXIMUM PRACTICAL ACCN. RATE, RADIAL EMITTANCE = $1.11\pi \times 10^{-4}$ m-rad.

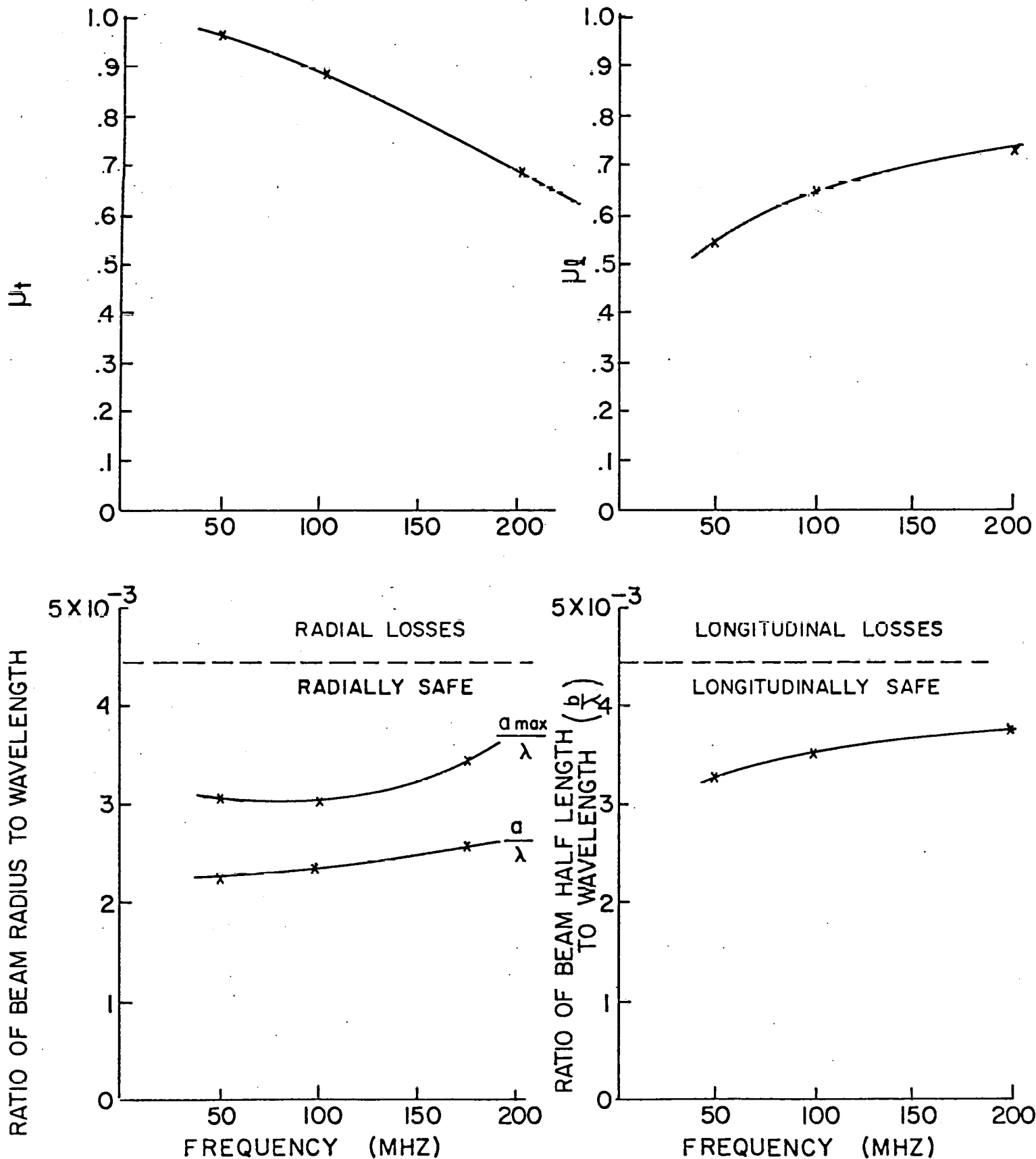


Figure 5

MATCHED BEAM PARAMETERS AS A FUNCTION OF BEAM CURRENT FOR DIFFERENT INITIAL QUADRUPOLE GRADIENTS. WITH + - + - QUADRUPOLE CONFIGURATION, MAGNET LENGTH / CELL LENGTH = 0.5, BORE RADIUS = 2.5 cm, $\lambda = 6m$, ACCELERATION RATE = 1 MeV/m, $\phi_s = 35^\circ$, LONGITUDINAL EMITTANCE = $6\pi \times 10^{-4}$ m-rad, RADIAL EMITTANCE = $1.3\pi \times 10^{-3}$ m-rad, (I = BEAM CURRENT IN AMPS), INJECTION ENERGY = 750 keV. DEUTERONS

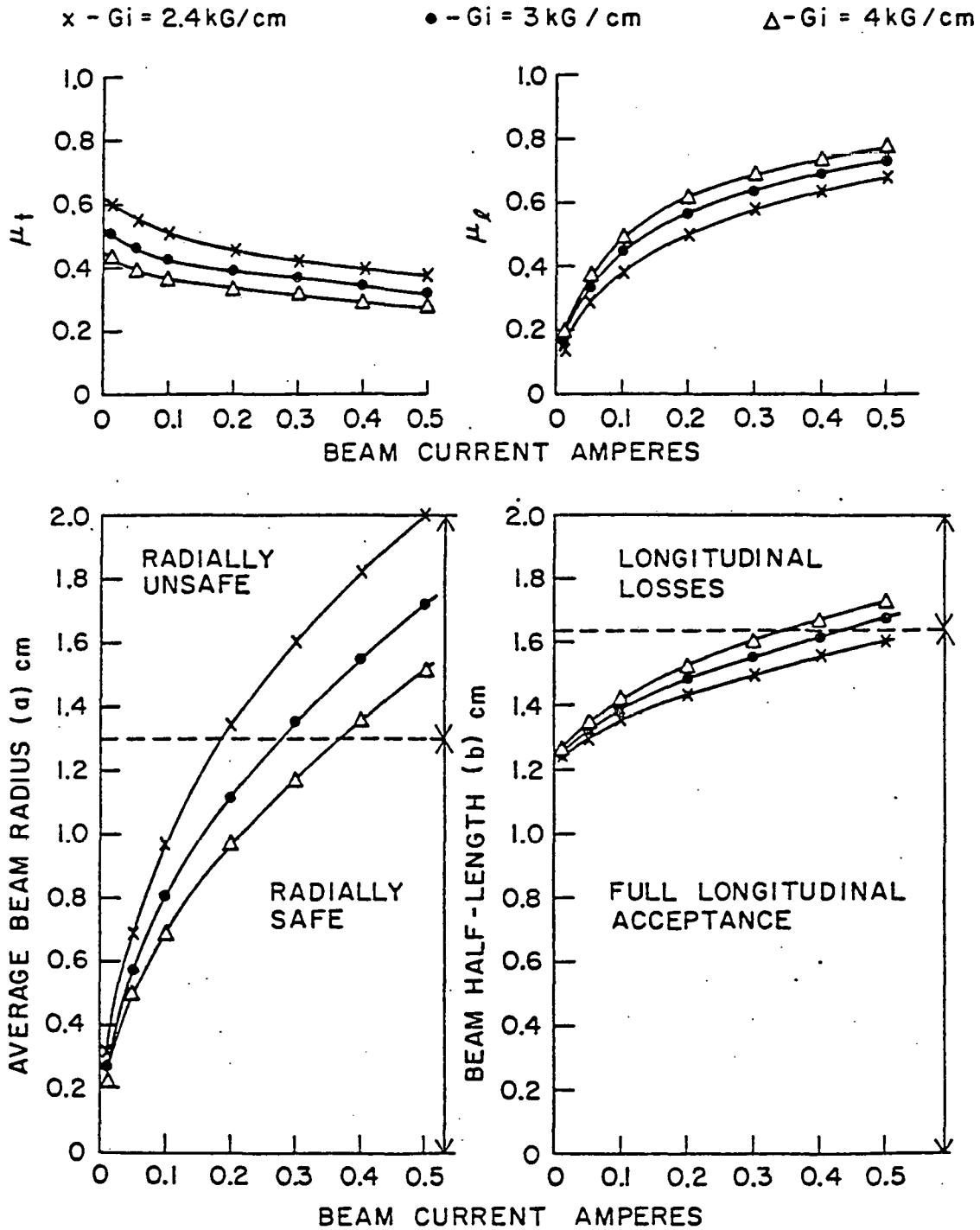


Figure 6

MATCHED BEAM PARAMETERS AS A FUNCTION OF BEAM CURRENT FOR 750 KeV PROTONS AND DIFFERENT INITIAL QUADRUPOLE GRADIENT WITH +-+ QUADRUPOLE CONFIGURATION. MAGNET/CELL LENGTH = 0.5, BORE RADIUS = 4 cm, $\lambda = 6$ m, ACCN. RATE = 0.8 MeV/m, $\phi_s = 40^\circ$, LONGITUDINAL EMITTANCE = $9.12 \pi \times 10^{-4}$ m-rad, RADIAL EMITTANCE = $3.7 (I_b) \pi \times 10^{-4}$ m-rad.

* Gi = 0.995 KG/cm

o Gi = 0.915 KG/cm

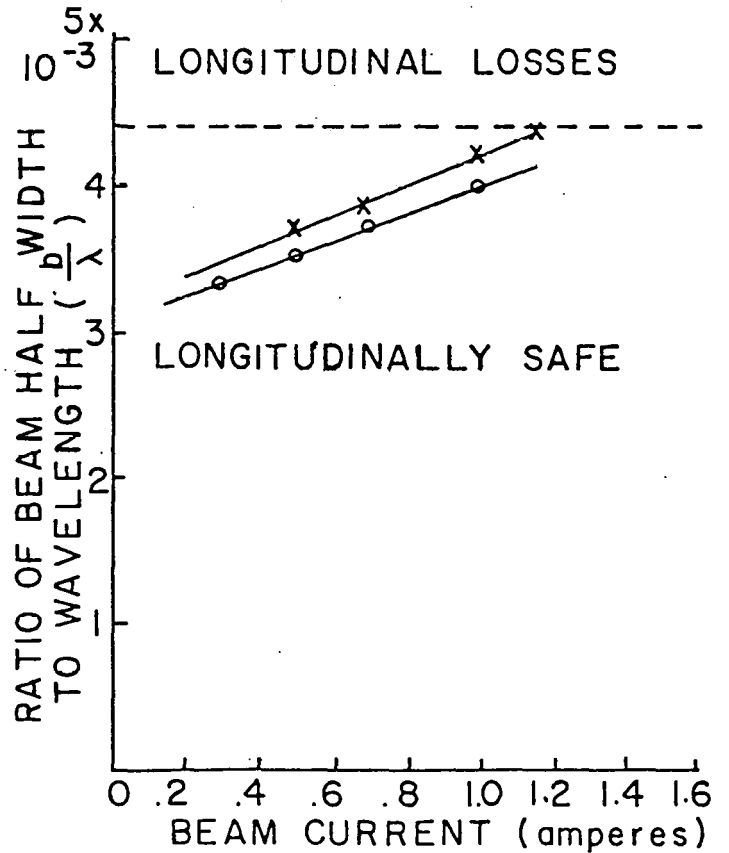
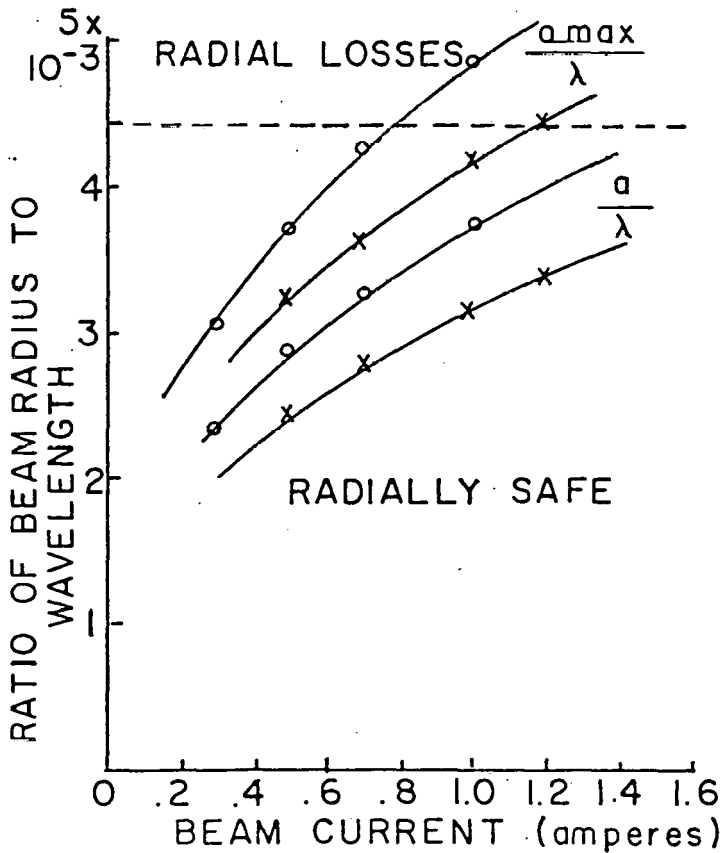
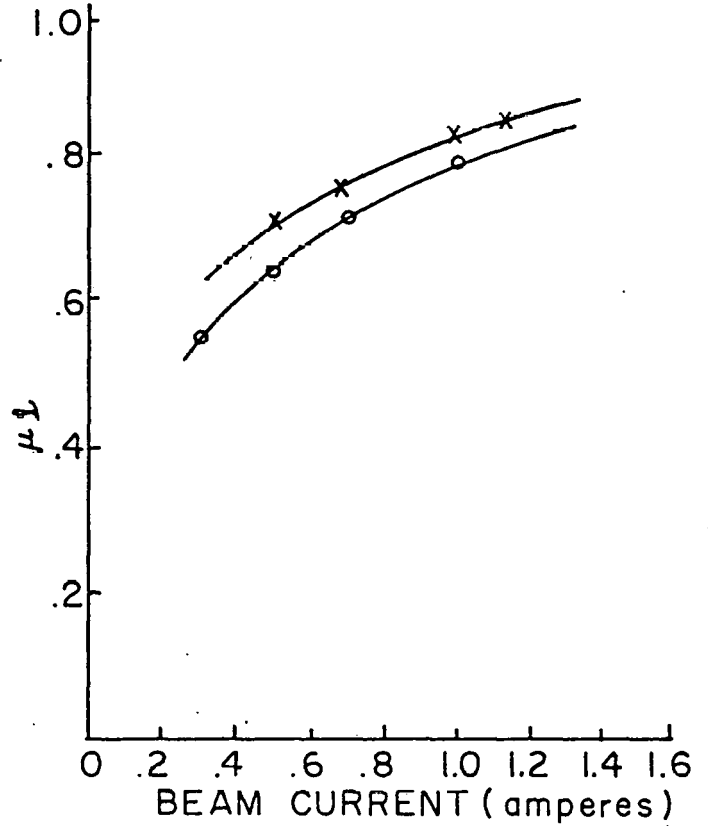
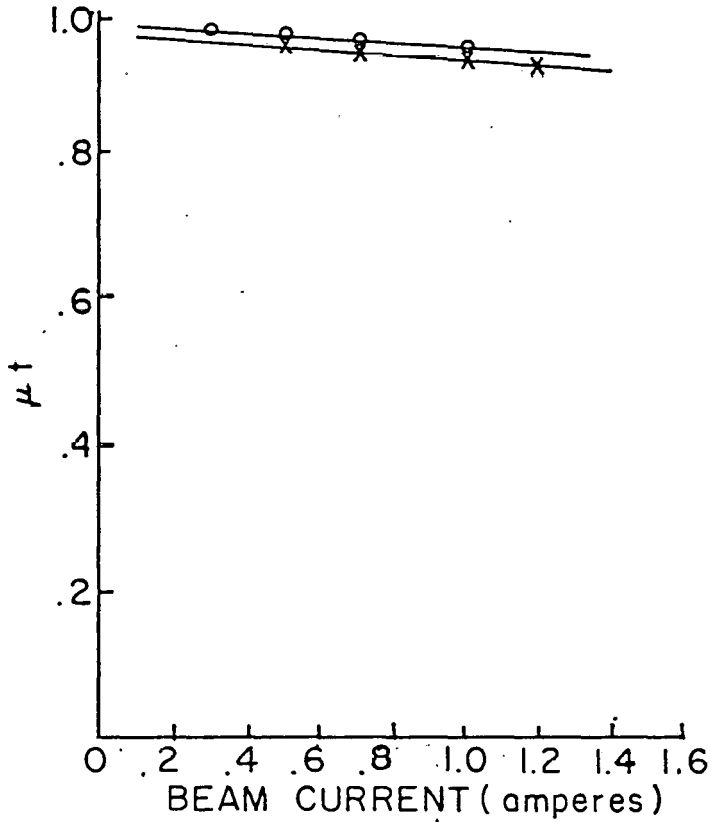


Figure 7

MATCHED BEAM PARAMETERS AS A FUNCTION OF LONGITUDINAL EMITTANCE FOR DIFFERENT INITIAL QUADRUPOLE GRADIENTS WITH $+--+$ QUADRUPOLE CONFIGURATION, MAGNET LENGTH / CELL LENGTH = 0.5, BORE RADIUS = 2.5 cm, $\lambda = 6m$, ACCELERATION RATE = 1Me V/m, $\phi_s = 35^\circ$, RADIAL EMITTANCE = $6\pi \times 10^{-4}$ m-rad, INJECTION ENERGY = 750 KeV, BEAM CURRENT = 0.2 AMPERES. DEUTERONS

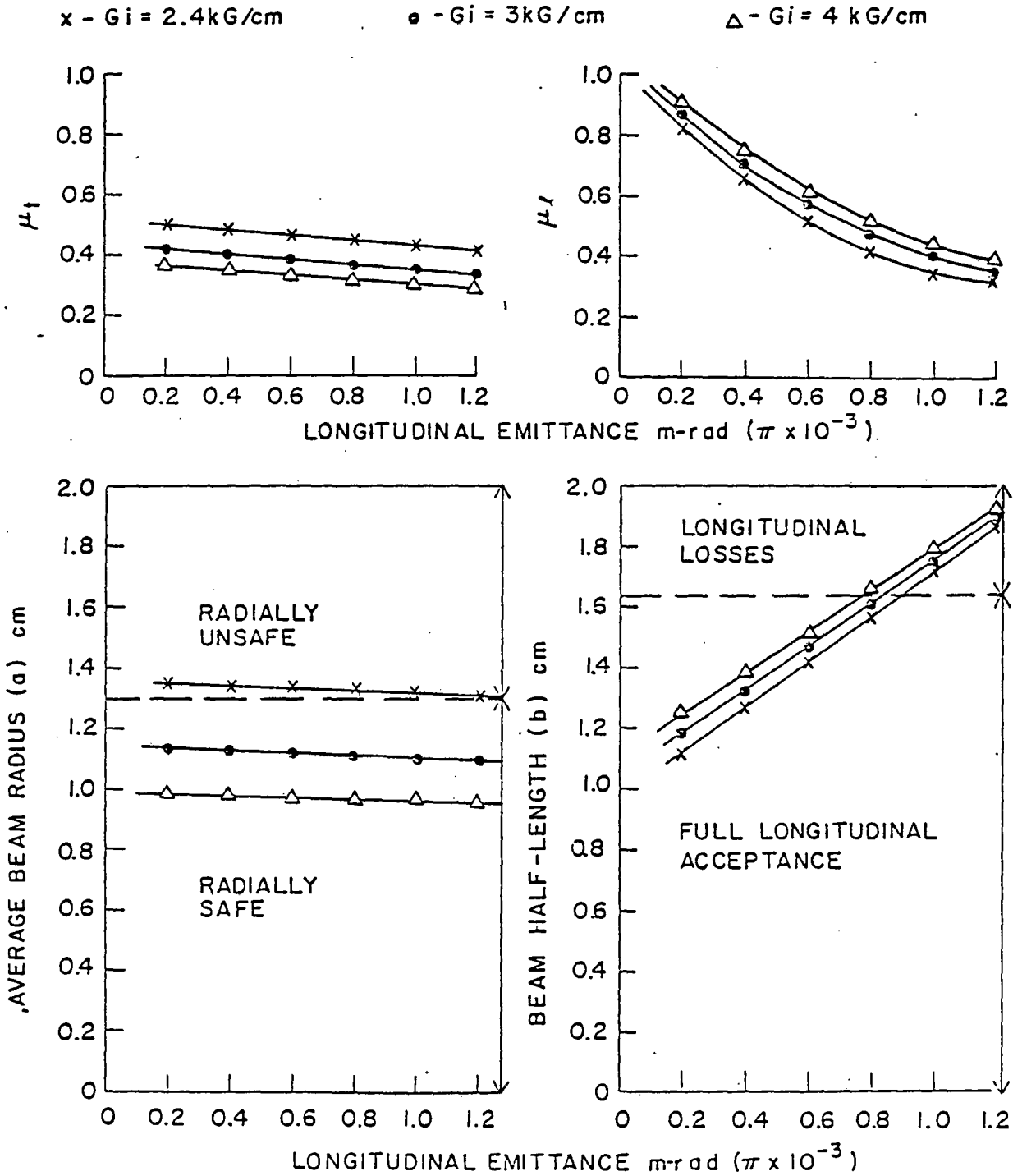


Figure 8

MATCHED BEAM PARAMETERS AS A FUNCTION OF RADIAL EMITTANCE FOR DIFFERENT INITIAL QUADRUPOLE GRADIENTS, WITH $+ - + -$ QUADRUPOLE CONFIGURATION, MAGNET LENGTH/CELL LENGTH = 0.5, BORE RADIUS = 2.5cm, $\lambda = 6$ m, ACCELERATION RATE = 1 MeV/m, $\phi_s = 35^\circ$, LONGITUDINAL EMITTANCE = $6\pi \times 10^{-4}$ m-rad, INJECTION ENERGY = 750KeV, BEAM CURRENT = 0.2 AMP. DEUTERONS

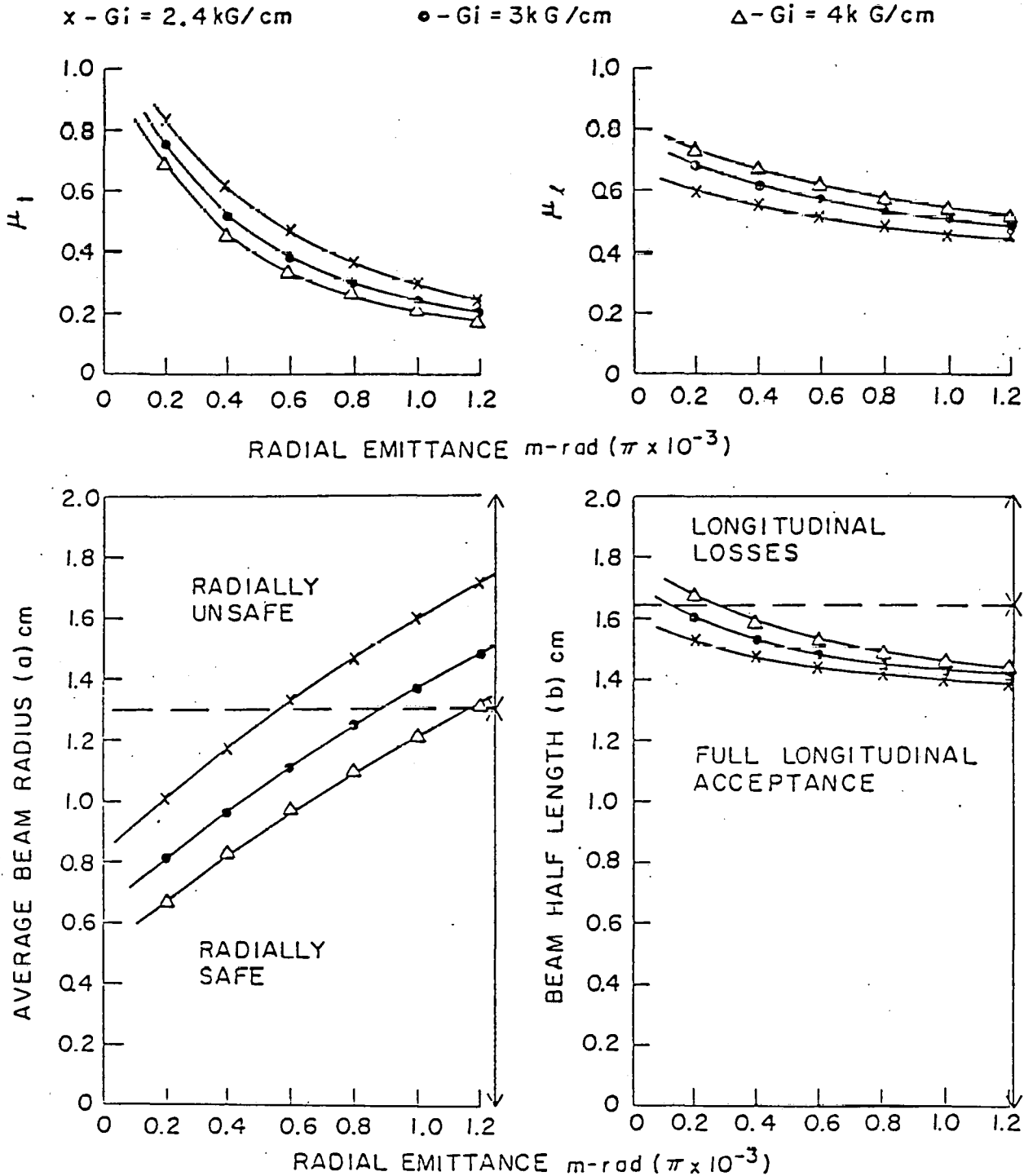


Figure 9

MATCHED BEAM PARAMETERS AS A FUNCTION OF LONGITUDINAL EMITTANCE FOR 750 KeV PROTON CURRENT OF 0.3 A FOR +--+ QUADRUPOLE CONFIGURATION AND CONSTANT PHASE ADVANCE PER MAGNET PERIOD OF $\mu_{sf} = \pi/2$, MAGNET/CELL LENGTH = 0.5, BORE RADIUS/WAVE LENGTH = 6.667×10^{-3} , $\phi_s = 40^\circ$, MAXIMUM PRACTICAL ACCELERATION RATE USED FOR EACH WAVELENGTH, RADIAL EMITTANCE = $1.11\pi \times 10^{-4}$ m-rad.

* - $\lambda = 150$ cm; $K = 1.6$ MeV/m; $G_i = 13.51$ KG/cm
 O - $\lambda = 300$ cm; $K = 1.12$ MeV/m; $G_i = 3.50$ KG/cm
 Δ - $\lambda = 600$ cm; $K = 0.8$ MeV/m; $G_i = 0.915$ KG/cm

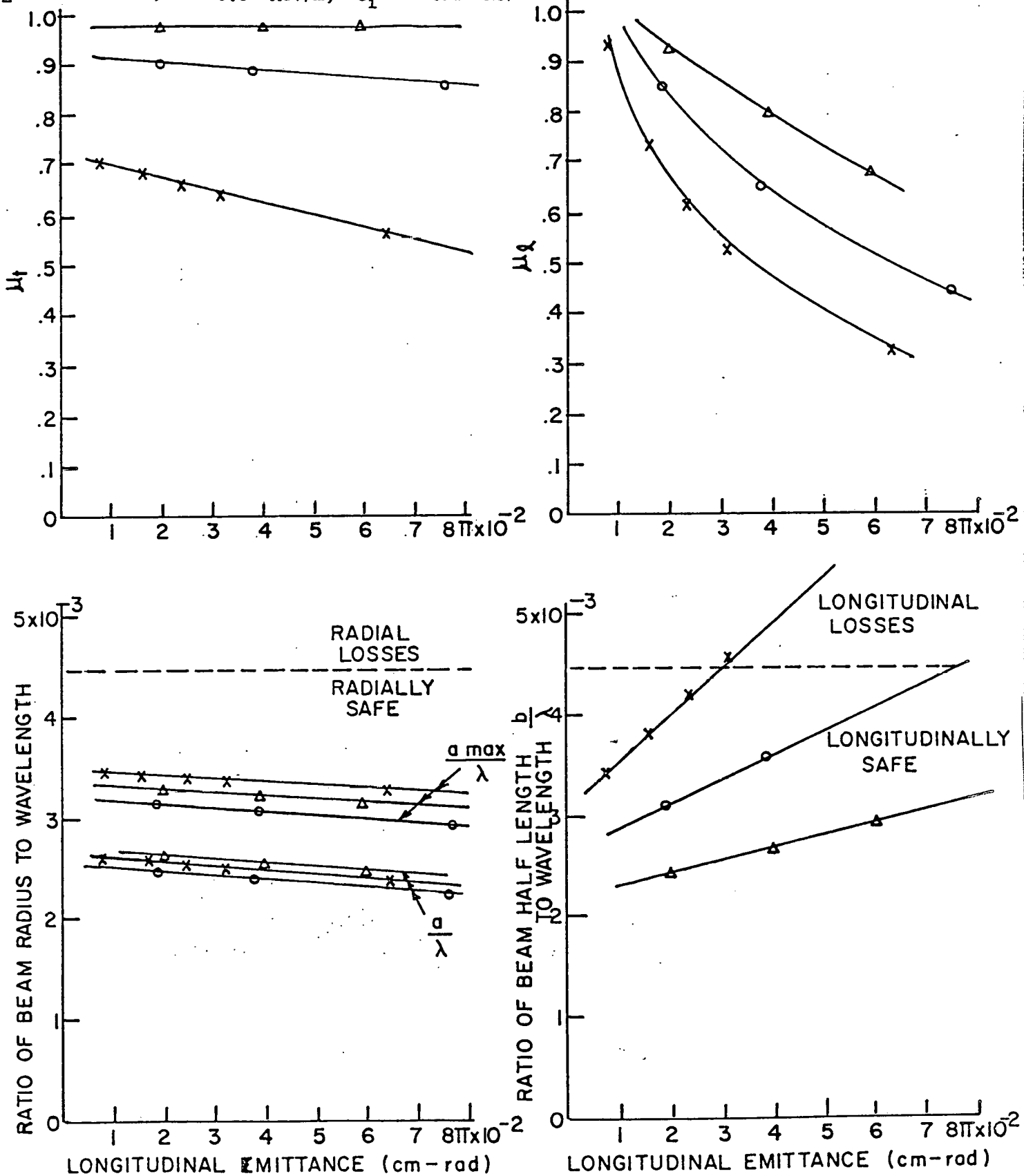


Figure 10

MATCHED BEAM PARAMETERS AS A FUNCTION OF RADIAL EMITTANCE FOR A 750-KeV PROTON CURRENT OF 0.3 A for +- QUADRUPOLE CONFIGURATION AND CONSTANT PHASE ADVANCE PER MAGNET PERIOD ($\mu s f = \pi/2$) MAGNET CELL LENGTH = 0.5. BORE RADIUS/WAVE LENGTH = 6.667×10^{-3} , $\phi_s = 40^\circ$ MAXIMUM PRACTICAL ACCELERATION RATE USED FOR EACH WAVE LENGTH.

* = LONGITUDINAL EMITTANCE = $1.61\pi \times 10^{-4}$ m-rad; $\lambda = 150$ cm; $K = 1.6$ MeV/m; $G_i = 13.51$ KG/cm
 @ = LONGITUDINAL EMITTANCE = $3.82\pi \times 10^{-4}$ m-rad; $\lambda = 300$ cm; $K = 1.12$ MeV/m; $G_i = 3.50$ KG/cm
 Δ = LONGITUDINAL EMITTANCE = $9.12\pi \times 10^{-4}$ m-rad; $\lambda = 600$ cm; $K = 0.8$ MeV/m; $G_i = 0.91$ KG/cm

